Trans. Phenom. Nano Micro Scales, 1(1): 1-18, Winter - Spring 2013
DOI: 10.7508/tpnms.2013.01.001

ORIGINAL RESEARCH PAPER

Natural Convection and Entropy Generation in Γ-Shaped Enclosure Using Lattice Boltzmann Method

E. Fattahi[1], M. Farhadi[1,*], K. Sedighi[1]
Faculty of Mechanical Engineering, Babol University of Technology Babol, Iran

Abstract

This work presents a numerical analysis of entropy generation in Γ-Shaped enclosure that was submitted to the natural convection process using a simple thermal lattice Boltzmann method (TLBM) with the Boussinesq approximation. A 2D thermal lattice Boltzmann method with 9 velocities, D2Q9, is used to solve the thermal flow problem. The simulations are performed at a constant Prandtl number (Pr = 0.71) and Rayleigh numbers ranging from 10^3 to 10^6 at the macroscopic scale (Kn = 10^{-4}). In every case, an appropriate value of the characteristic velocity i.e. V D $\sqrt{bg_y \quad TH}$ is chosen using a simple model based on the kinetic theory. By considering the obtained dimensionless velocity and temperature values, the distributions of entropy generation due to heat transfer and fluid friction are determined. It is found that for an enclosure with high value of Rayleigh number (i.e., Ra=10^5), the total entropy generation due to fluid friction and total Nu number increases with decreasing the aspect ratio.

Keywords: *Entropy Generation; Lattice Boltzmann Method; Natural Convection; Γ-Shaped enclosure*

1. Introduction

The lattice Boltzmann (LB) method is a powerful approach to hydrodynamics, with applications ranging for vast Reynolds numbers and modeling the physics in fluids [1–4]. Various numerical simulations have been performed using different thermal LB models or Boltzmann-based schemes to investigate the natural convection problems [5–11].
The lattice Boltzmann equation (LBE) is a minimal form of the Boltzmann kinetic equation, and the result is a very elegant and simple evolution equation for a number of distribution functions, which represent the number of fluid particles moving in these discrete with speed c_i .In LBM the domain is discretized in uniform Cartesian cells which each one holds a fixed directions. With respect to the more conventional numerical methods commonly used for the study of fluid

flow situations, the kinetic nature of LBM (Lattice Boltzmann Method) introduces several advantages, including easy implementation of boundary conditions and fully parallel algorithms. In addition, the convection operator ($\vec{c}.\nabla \vec{f}$) is linear, no Poisson equation for the pressure must be solved and the translation of the microscopic distribution function into the macroscopic quantities consists of simple arithmetic calculations. The phenomenon of natural convection in enclosures has attracted increasing attention in recent years.

*Corresponding author
Email Address: mfarhadi@nit.ac.ir

Nomenclature

		T_h	Hot temperature (K)
c_i	Discrete lattice velocity in direction (i)	T_c	Cold temperature (K)
c_s	Speed of sound in Lattice scale	T_0	Bulk temperature (K), (T_0= (T_h+T_c)/2)
F_i	External force in direction of lattice velocity	u, v	Horizontal and vertical components of velocity
f_i^{eq}	Equilibrium distribution		$(m.s^{-1})$
g_y	Acceleration due to gravity, $(m.s^{-2})$	w_k	Weighting factor
H	Height of enclosure (m)	w	non-dimensional length of step, (w′/ H)
h	Non-dimensional height of step, (h′/H)		
k	Thermal conductivity $(W.m^{-1}.K^{-1})$		**Greek symbols**
$\overline{Nu}$	Mean Nusselt number	β	Thermal expansion coefficient $\left(K^{-1}\right)$
Nu_x, Nu_y	Local Nusselt number along surfaces	μ	Molecular viscosity $(kg.m^{-1}.s^{-1})$
Pr	Prandtl number (ν/α)	φ	Irreversibility distribution ratio
Ra	Rayleigh number $(g\beta\Delta TH^3/\alpha\nu)$	ρ	Density $(kg.m^{-3})$
Kn	Knudsen number	τ	Lattice relaxation time
S'''_{gen}	Total volumetric entropy generation rate $\left(W.m^{-3}.K^{-1}\right)$	Δt	Lattice time step
S'''_P	Volumetric entropy generation rate due to friction $\left(W.m^{-3}.K^{-1}\right)$		**Subscript**
		C	cold
S'''_T	Volumetric entropy generation rate due to heat transfer $\left(W.m^{-3}.K^{-1}\right)$	h	hot
		i	discrete lattice directions

Applications extending from the double paned windows in buildings to the cooling of electronic systems are examples of natural convection systems. In natural convection processes, the thermal and the hydrodynamic are coupled and both are, according to Bejan [12], strongly influenced by the fluid thermo-physical characteristics, the temperature differences and the system geometry. The comprehensive reviews of articles on natural convection were made by Catton [13], Ostrach [14] and Kakac and Yener [15]. In addition to the studies [16-20], Lage and Bejan [21] investigated numerically the natural convection in a square enclosure heated and cooled in the horizontal direction in the Prandtl number range 0.01– 10 and the Rayleigh number range 10^2 –10^{11}. Notable researches have been done to investigate importance of entropy generation in thermal systems. Entropy generation and its minimization were investigated widely with Bejan [22-24]. Natural convection in enclosure was summarized in rectangular coordinates by Davis [25]. In his study, he made a review about numerical studies and investigated the effect of various non-dimensional numbers and boundary conditions on natural convection heat transfer. Additionally, an analysis of the entropy generation in rectangular cavities was

performed by Oliveski et al. [26]. They found that for the same aspect ratio, the entropy generation due to the viscous effects increases with the Rayleigh number and, for a certain Rayleigh number, the entropy generation due to the viscous effects also increases with the aspect ratio.

Ha and Jung [27] used LBM to investigate the steady, three-dimensional, conjugate heat transfer of natural convection and conduction in a vertical cubic enclosure within which a centered, cubic, heat-conducting body generates heat. They found that the fluid flow and temperature distribution show very complex three-dimensional pattern. Mezrhab et al. [28] studied the radiation-natural convection interactions of a square heat-conduction body within a differentially heated square cavity. Dagtekin et al. [29] dealt with the prediction of entropy generation of natural convection in a Γ-shaped enclosure using FDM (Finite Difference Method). They found that the main entropy generation is formed due to heat transfer for $Ra<10^5$, while the contribution due to fluid friction becomes stronger for $Ra>10^5$.

In the present study natural convection and entropy generation was simulated numerically in the Γ-shaped enclosure using LBM. As the horizontal walls are insulated perfectly, vertical walls heats. An in house lattice BGK (Bhatnagar–Gross–Krook) scheme FORTRAN code was used to simulate the present problem. The contribution of this work is the analyses of the variation of entropy generation in relation to Rayleigh number, aspect ratio at fixed irreversibility coefficient($\phi=10^{-6}$) in Γ-shaped enclosure. The results are displayed graphically in term of the streamlines, isotherms and local entropy generation contours to show the effect of aspect ratio (AR) and Rayleigh number. To calculate the entropy generation, a new model [30] was used to determine the dimensionless velocity. The results of the present study show that this model is a suitable for calculating the entropy generation in the natural convection problems.

2. Numerical Procedure

2.1 The Lattice Boltzmann Method

In investigating the natural convection problems, the effect of viscous heat dissipation can be neglected for applications in incompressible flow [10]. This assumption can be used to simulate the natural convection by LBM. The LB model used here is the same as that employed in [9-11]. The thermal LB model utilizes two distribution functions, f and g, for the flow and the temperature field, respectively. It uses modeling of movement of fluid particles to capture macroscopic fluid quantities such as velocity, pressure and temperature. In this approach the fluid domain is discretized in uniform Cartesian cells. Each cell holds a fixed number of distribution functions, which represent the number of fluid particles moving in specified discrete directions. For this work, the most popular model for the 2D case, the D2Q9 model, which consists of 9 distribution functions, has been used (Fig. 1). The values of $w_0 = 4/9$ for $|c_0| = 0$ (for the static particle), $w_{1-4} = 1/9$ for $|c_{1-4}| = 1$ and $w_{5-9} = 1/36$ for $|c_{5-9}| = \sqrt{2}$ are assigned for this model.

The density and distribution functions i.e. the f and g (temperature distribution function), are calculated by solving the Lattice Boltzmann equation (LBE), which is a special discretization of the kinetic Boltzmann equation. After introducing BGK approximation, the general form of lattice Boltzmann equation with external force can be written as:

$$f_i(x + c_i\Delta t, t + \Delta t) = f_i(x,t) + \frac{\Delta t}{\tau_v}\left[f_i^{eq}(x,t) - f_i(x,t)\right] + \Delta t c_i . F_i \quad (1)$$

For the flow field and

$$g_i(x + c_i\Delta t, t + \Delta t) = g_i(x,t) + \frac{\Delta t}{\tau_D}\left[g_i^{eq}(x,t) - g_i(x,t)\right] \quad (2)$$

For the temperature field

Where Δt denotes lattice time step, c_i is the discrete lattice velocity in direction k , F_i is the external force in direction of lattice velocity, τ_v and τ_D denotes the lattice relaxation time for the flow and temperature field. The kinetic viscosity υ and the thermal diffusivity α, are defined in terms of their respective relaxation times, i.e. $\upsilon = c_s^2(\tau_v - 1/2)$ and $\alpha = c_s^2(\tau_D - 1/2)$, respectively. The speed of sound (c_s) is a lattice-dependent quantity, which has the value of $1/\sqrt{3}$ for the D2Q9 model. Note that the

limitation $0.5 < \tau$ should be satisfied for both relaxation times to ensure that viscosity and thermal diffusivity are positive. Furthermore, the local equilibrium distribution functions are calculated with equations (3, 4) for the flow and temperature fields, respectively.

$$f_i^{eq} = w_i . \rho . \left[1 + \frac{c_i \vec{u}}{c_s^2} + \frac{1}{2} \frac{(c_i \vec{u})^2}{c_s^4} - \frac{1}{2} \frac{\vec{u}\vec{u}}{c_s^2} \right] \quad (3)$$

$$g_i^{eq} = w_i T(x,t) . \left[1 + \frac{c_i \vec{u}}{c_s^2} \right] \quad (4)$$

Where w_i a weighting factor, $\vec{u}$ is velocity vector and ρ is the lattice fluid density.

In order to incorporate buoyancy force in the model, the force term in the equation (1) need to be calculated as below in vertical direction (y) [31]:

$$F_i = 3 w_i g_y \beta \theta \quad (5)$$

The Boussinesq approximation is applied and radiation heat transfer is negligible. θ is non-dimensional temperature.

To ensure that the code works in near incompressible regime, the characteristic velocity of the flow $V \equiv \sqrt{\beta g_y \Delta T H}$ must be small compared with the fluid speed of sound. In the present study, the characteristic velocity was selected as 0.1 of speed of sound.

Finally, the following macroscopic variables can be calculated in terms of these variables, with the following formula.

Flow density: $$\rho = \sum_i f_i \quad (6)$$

Momentum: $$\rho u_i = \sum_j f_j c_{ji} \quad (7)$$

Temperature: $$T = \sum_i g_i \quad (8)$$

2.2 Entropy Generation Calculation

The following dimensionless variables (primed quantities are dimensional) are used:

$$(x, y) = (x', y')/H, \quad u, v = (u', v')H/\alpha,$$
$$T = (T' - T_c)/\Delta T, \ \Delta T = T_h - T_c, Pr = \upsilon/\alpha \quad (9)$$

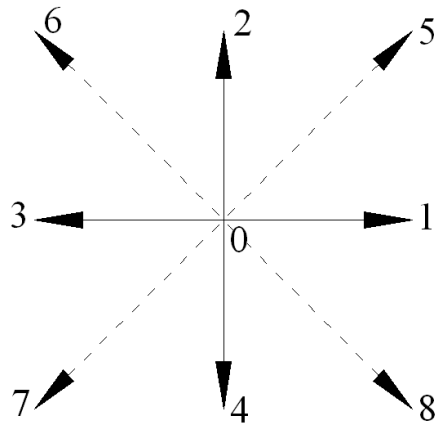


Fig. 1. Discrete velocity vectors for the D2Q9 model of LBM

Volumetric entropy generation due to heat transfer, S_T''', and friction, S_P''', are calculated as below:

$$S_T''' = \frac{k}{T^2} (|\nabla T|)^2 \quad (10)$$

$$S_P''' = \frac{\mu}{T} \psi \quad (11)$$

where ψ is defined by:

$$\psi = \left(\frac{\partial u_i}{\partial x_j} + \frac{\partial u_j}{\partial x_i} \right) \frac{\partial u_i}{\partial x_j} \quad (12)$$

And the total volumetric entropy generation can be obtained by:

$$S_{gen}''' = S_T''' + S_P''' \quad (13)$$

The dimensionless form of Eq. (13) is called Ns (local EG number) which is defined as follow:

$$Ns = \underbrace{\left[\left(\frac{\partial T}{\partial x} \right)^2 + \left(\frac{\partial T}{\partial y} \right)^2 \right]}_{S_T} + \underbrace{\phi \left[2 \left(\frac{\partial u}{\partial x} \right)^2 + \left(\frac{\partial v}{\partial y} \right)^2 + \left[\left(\frac{\partial v}{\partial x} + \frac{\partial u}{\partial y} \right)^2 \right] \right]}_{S_P} \quad (14)$$

The irreversibility distribution ratio, ϕ (the ratio of entropy generated due to fluid friction to heat transfer), is written as follows:

$$\phi = \frac{\mu T_0}{k}\left(\frac{\alpha}{H\,\Delta T}\right)^2 \tag{15}$$

T_0 is bulk temperature ($T_0 = (T_h + T_c)/2$ (K). The dimensionless total entropy generation is the integral volume of the computational domain:

$$S = \int_v N_s dV \tag{16}$$

2.3 Curved Boundary Treatment

Consider Fig. 2 is a part of an arbitrary curved wall geometry, where the black small circles on the boundary $\mathbf{x}_w$, the open circles represent the boundary nodes in the fluid region $\mathbf{x}_f$ and the grey circles indicate those in the solid region $\mathbf{x}_b$ .In the boundary condition $\tilde{f}(\mathbf{x}_b, t), \tilde{g}(\mathbf{x}_b, t)$ are needed to perform the streaming steps on fluid nodes $\mathbf{x}_f$.

The fraction of an intersected link in the fluid region Δ is defined by:

$$\Delta = \frac{\left\|\mathbf{x}_f - \mathbf{x}_w\right\|}{\left\|\mathbf{x}_f - \mathbf{x}_b\right\|} \tag{17}$$

The standard (half-way) bounce back no-slip boundary condition always assumes a delta value of 0.5 to the boundary wall (Fig.3a). Due to the curved boundaries, delta values in the interval of (0, 1] are now possible. Fig.3b shows the bounce back behavior of a surface with a delta value smaller than 0.5 and Fig.3c shows the bounce back behavior of a wall with delta bigger than 0.5. In all three cases, the reflected distribution function $\tilde{f}_{\bar{\alpha}}(\mathbf{x}, t+\Delta t)$ at $\mathbf{x}_f$ is unknown. Since the fluid particles in the LBM are always considered to move one cell length per time step, the fluid particles would come to rest at an intermediate node $\mathbf{x}_i$. In order to calculate the reflected distribution function in node $\mathbf{x}_f$, an interpolation scheme has to be applied. For treating velocity field in curved boundaries, the method is based on the method reported in [32]. For temperature field, the method is based on an extrapolation method of second-order accuracy applied in [33].

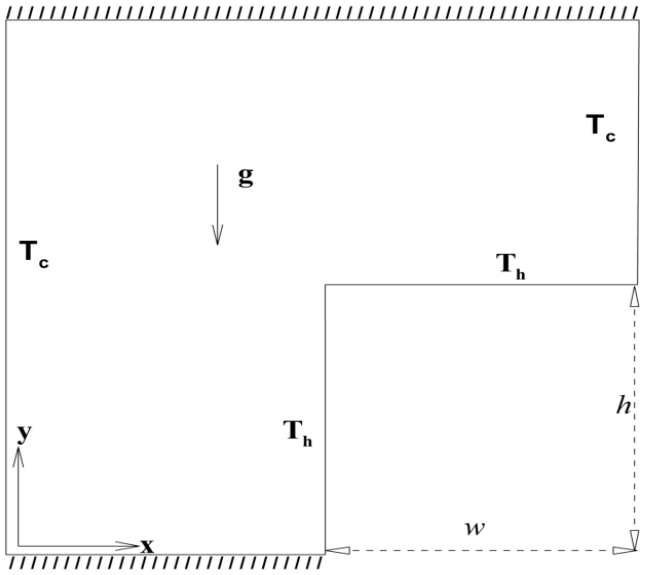


Fig. 2. Schematic view of Γ-shaped enclosure

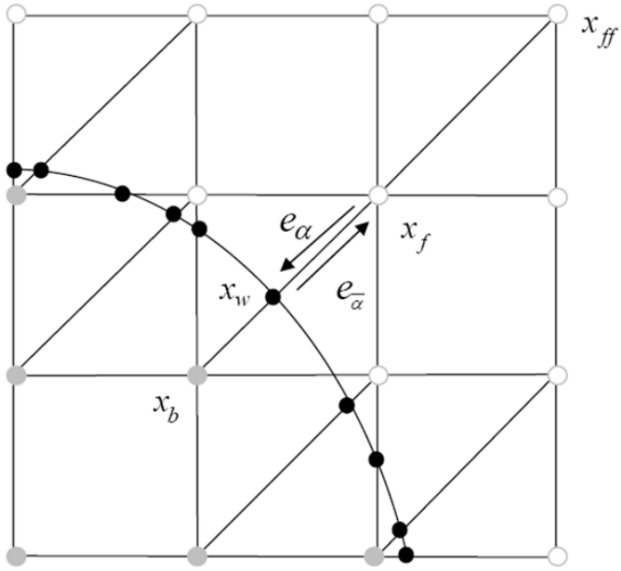


Fig. 3. Layout of the regularly spaced lattices and curved wall boundary

2.3.1 Velocity in curved boundary condition

To calculate the distribution function in the solid region $\tilde{f}_{\bar{\alpha}}(\mathbf{x}_b, t)$ based upon the boundary nodes in the fluid region, the bounce-back boundary conditions combined with interpolations including a one-half grid spacing correction at the boundaries [3, 34].

Then the Chapman–Enskog expansion for the post-collision distribution function on the streaming step is conducted as:

$$\begin{aligned}\tilde{f}_{\bar{\alpha}}(\mathbf{x}_b,t+\Delta t)&=(1-\lambda)\tilde{f}_{\alpha}(\mathbf{x}_f,t+\Delta t)\\&+\lambda f_{\alpha}^{o}(\mathbf{x}_b,t+\Delta t)\\&-2\frac{3}{c^2}w_{\alpha}\rho(\mathbf{x}_f,t+\Delta t)\mathbf{e}_{\alpha}.\mathbf{u}_w\end{aligned} \tag{18}$$

Where

$$\begin{aligned}f_{\alpha}^{o}(\mathbf{x}_b,t+\Delta t)&=f_{\alpha}^{eq}(\mathbf{x}_f,t+\Delta t)\\&+\frac{3}{c^2}w_{\alpha}\rho(\mathbf{x}_f,t+\Delta t)\mathbf{e}_{\alpha}.\left(\mathbf{u}_{bf}-\mathbf{u}_f\right)\end{aligned} \tag{19}$$

$$\mathbf{u}_{bf}=\mathbf{u}_{ff},\quad \lambda=\frac{2\Delta-1}{\tau_m-2},\ \ if\ \ 0<\Delta\le\frac{1}{2} \tag{20a}$$

$$\mathbf{u}_{bf}=(1-\frac{3}{2\Delta})\mathbf{u}_f+\frac{3}{2\Delta}\mathbf{u}_w,\quad \lambda=\frac{2\Delta-1}{\tau_m+\frac{1}{2}},\ \ if\ \ \frac{1}{2}<\Delta\le 1 \tag{20b}$$

$\mathbf{u}_w$ denotes the velocity of solid wall, $\mathbf{u}_{bf}$ is the imaginary velocity for interpolations and $\mathbf{e}_{\bar{\alpha}}\equiv-\mathbf{e}_{\alpha}$.

Temperature in curved boundary condition

For temperature field in curved boundary this study use the method is based on the method reported in [34]. Distribution function for temperature divided two parts, equilibrium and non equilibrium

$$g_{\bar{\alpha}}(\mathbf{x}_b,t)=g_{\bar{\alpha}}^{eq}(\mathbf{x}_b,t)+g_{\bar{\alpha}}^{neq}(\mathbf{x}_b,t) \tag{21}$$

By substituting Eq.21 into temperature streaming step, we have

$$\begin{aligned}\tilde{g}_{\bar{\alpha}}(\mathbf{x}_b,t+\Delta t)&=g_{\bar{\alpha}}^{eq}(\mathbf{x}_b,t)\\&+(1-\frac{1}{\tau_T})g_{\bar{\alpha}}^{neq}(\mathbf{x}_b,t)\end{aligned} \tag{22}$$

Obviously to calculate $\tilde{g}_{\alpha}(\mathbf{x}_b,t+\Delta t)$, both $g_{\alpha}^{eq}(\mathbf{x}_b,t)$ and $g_{\alpha}^{neq}(\mathbf{x}_b,t)$ are required.

Equilibrium and non equilibrium parts of Eq.21 are define as:

$$g_{\bar{\alpha}}^{eq}(\mathbf{x}_b,t)=w_{\bar{\alpha}}T_b^{*}\left(1+\frac{3}{c^2}\mathbf{e}_{\bar{\alpha}}.\mathbf{u}_b\right) \tag{23}$$

T_b^{*} is determined by linear extrapolation using either:

$$T_b^{*}=T_{b1},\qquad \text{if } \Delta\ge 0.75 \tag{24a}$$

$$T_b^{*}=T_{b1}+(1-\Delta)T_{b2},\ \text{if } \Delta\le 0.75 \tag{24b}$$

Where Δ is the fraction of the intersected link in the fluid region (Eq. 17), which is illustrated in Fig. 3 and:

$$T_{b1}=[T_w+(\Delta-1)T_f]/\Delta \tag{25a}$$

$$T_{b2}=[2T_w+(\Delta-1)T_{ff}]/(1+\Delta) \tag{25b}$$

Where T_f and T_{ff} denote the fluid temperatures in node x_f and x_{ff}, respectively. The extrapolation scheme is the same as Ref. [35].

The next task is to determine the $g_{\alpha}^{neq}(\mathbf{x}_b,t)$. Second-order approximation is also used. $g_{\alpha}^{neq}(\mathbf{x}_b,t)$ is evaluated as:

$$\begin{aligned}g_{\alpha}^{neq}(\mathbf{x}_b,t)&=\Delta g_{\alpha}^{neq}(x_f,t)\\&+(1-\Delta)g_{\alpha}^{neq}(x_{ff},t)\end{aligned} \tag{26}$$

From the Chapman-Enskog analysis, $g_{\alpha}^{neq}(\mathbf{x},t)$ can be expressed as:

$$g_{\alpha}^{neq}(\mathbf{x},t)=g_{\alpha}^{1}(\mathbf{x},t)\delta x. \tag{27}$$

Where $g_{\alpha}^{0}(\mathbf{x},t)$ is the same order as $g_{\alpha}^{eq}(\mathbf{x},t)$. Since

$$g_{\alpha}^{1}(\mathbf{x_w},t)-g_{\alpha}^{1}(\mathbf{x_f},t)=O(\delta x),$$

$$g_{\alpha}^{neq}(\mathbf{x_w},t)-g_{\alpha}^{neq}(\mathbf{x_f},t)=O(\delta x^2).$$

By the same token, it can be proved that

$$g_{\alpha}^{neq}(\mathbf{x_w},t)-g_{\alpha}^{neq}(\mathbf{x_{ff}},t)=O(\delta x^2) \tag{28}$$

That means the approximation $g_{\alpha}^{neq}(\mathbf{x}_b,t)$ is of second order in space which is in consistent with thermal lattice Boltzmann equation.

3.2. Computational Domain and Numerical Details

Figure 4 shows the Γ-Shaped enclosure analyzed in the present study. h, w, AR are the height of the step, the width of the step and the aspect ratio (h/w), respectively. The step heater kept at a constant temperature of T_h and the vertical walls of the enclosure are fixed at low isothermal of T_c. The top and bottom walls are insulated.

No-slip boundary condition was imposed on all the walls of the cavity. Dirichlet type boundary conditions have been used that the insulated boundary conditions were simulated by converting them to Dirichlet type by using a second order accurate finite-difference approximation. The boundary conditions have been implemented by using the counter-slip approach such as Dixit and Babu [8]. Although the suitability of the counter slip approach has only been established for the hydrodynamic boundary conditions [36], but Dixit and Babu [8] have shown that this technique is useful for modeling the thermal boundary conditions to simulate the flow and heat transfer in the cavity. They found that "the traditional implementation of the Dirichlet boundary condition gave rise to a spurious gradient in the temperature between the wall and the first point in the fluid. This gradient was a steep drop in the temperature near the hot wall and the cold wall and it persisted even after decreasing the mesh spacing by a factor of 8. This clearly implies that the source of this phenomenon is the implementation of the boundary condition and not the grid spacing especially for a lower value of Rayleigh number. This, in turn, would yield incorrect values of wall Nusselt number. To overcome this difficulty, the counter-slip approach has been used for simulating the Dirichlet boundary condition also". This method was investigated carefully in detail by Dixit [37]. As mentioned above, this boundary condition was used on the walls of the cavity.

The Rayleigh number (Ra) and Nusselt number (Nu) for the current problem are defined as follow:

$$Ra = g\beta\Delta TH^3/\alpha\upsilon \tag{29}$$

Local Nusselt numbers are defined on front and top face of the step as Nu_x, Nu_y

$$Nu_x = -\left(\frac{\partial T}{\partial x}\right)_h, \qquad Nu_y = -\left(\frac{\partial T}{\partial y}\right)_w \tag{30}$$

The average Nusselt number is calculated by integrating the local Nusselt number along surface of step as**:**

$$\bar{Nu} = \frac{1}{h+w}\left[\int_0^h Nu_y dy + \int_0^w Nu_x dx\right] \tag{31}$$

Determination of characteristic velocity is necessary to simulate the natural convection in LBM. This velocity is defined as $V \equiv \sqrt{\beta g_y \Delta TH}$. The kinetic viscosity and thermal diffusivity are calculated from the characteristic velocity through the following relationships, respectively:

$$\upsilon^2 = \frac{V^2 H^2 \Pr}{Ra}$$

and (31)

$$\alpha = \frac{\upsilon}{\Pr}$$

The relaxation times, τ_υ and τ_D, for flow and temperature LB equations given in equation (1) and (2) can then be determined. It implies that kinetic viscosity (υ) and thermal diffusivity (α) can not be considered as constants in LBM simulations if the characteristic velocity (V) is kept constant. Kao et al. [38] developed a new model for determining an appropriate characteristic velocity value based on the principle of kinetic theory. From the kinetic theory [39, 40], the Knudsen number is defined as [41]:

$$Kn = \sqrt{\frac{\pi\gamma}{2}}.\frac{Ma}{\mathrm{Re}} \tag{32}$$

Where Ma is the Mach number, Re is the Reynolds number, and the heat capacity ratio to be γ = 5/3 for a monatomic ideal gas and γ = 7/5 for a diatomic gas according to the definition of mean free path, $\lambda = \sqrt{\frac{\pi\gamma}{2}}\frac{\upsilon}{c_s}$, the Knudsen number for this geometry can be written as [38]:

$$Kn \equiv \frac{\lambda}{H} = \sqrt{\frac{\pi\gamma}{2}}.\frac{v}{c_s.H} \tag{33}$$

From the definition of Rayleigh number and Eq (17):

$$V^2 = \frac{Ra.Kn^2.c_s^2}{\pi\gamma\Pr/2}, \text{where } c_s^2 = \frac{c^2}{3} \tag{34}$$

By this definition, the characteristic velocity is a function of the Rayleigh number, Knudsen number,

Prandtl number and the value of *c*, that all are specified as a given values in LBM simulations which includes the macroscopic and mesoscopic scales at natural convection problems.

For grid independency, the average Nusselt number over the step was calculated at high Ra numbers for different grid points. As seen in table 1 for grid points passing from 80×80 and 100×100 for Ra = 10^5 and 10^6, respectively, no considerably change in the average Nusselt number was observed (maximum variation is less then 0.16%). According to the table 1, the 80×80 grid points was used for Ra ≤ 10^5 and 100×100 grid points was used only for Ra = 10^6.

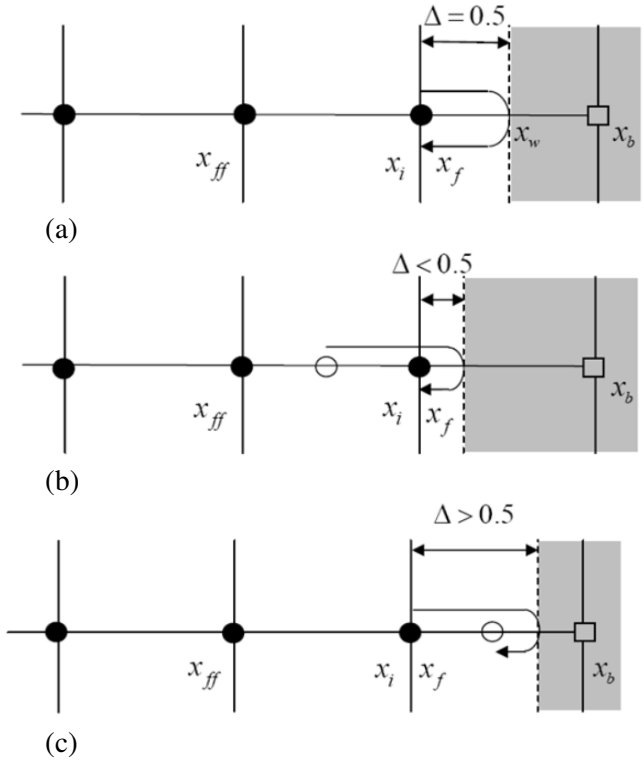


Fig. 4. Illustration of the bounce-back boundary conditions. (a) Δ = 1/2, the ‘‘perfect” bounce-back without interpolation. (b) Δ < 1/2, the bounce-back with interpolations before the collision with the wall located at x_w. (c) Δ > 1/2, the bounce-back with interpolations after the collision with the wall

5. Results and discussion

To validate the numerical simulation, the results of natural convection in square and Γ-shaped enclosure were compared with previous works ([25] and [29]).

In the square cavity, flow was heated from the left wall, while the right wall was maintained at a constant low temperature. Meanwhile, the upper and bottom walls were assigned adiabatic boundary conditions. A vertical gravitational effect was applied in the y-direction. Regarding the flow field, the square cavity was assumed to be closed and the no-slip boundary conditions were imposed at each of the four solid walls. In this simulations, appropriate values of V were obtained using the model presented in Eq. (23) with a fixed Knudsen number of Kn = 10^{-4} at the macroscopic scale and Rayleigh numbers of Ra = 10^5 and 10^6, respectively.

The results of the present simulation in comparison with the previous study ([25]) are shown in the table 2. The results of the present study show a good agreement (maximum variation is less than 2%) with the previous study.

Figure 5 shows the temperature contours and streamlines in the Γ-shaped enclosure in comparison with the results of the FDM [29]. The results show a good accuracy of present simulation. As mentioned above, this model is a suitable technique for simulation of fluid flow and heat transfer in natural convection problems using LBM in the cavity. On the other hand, to validate the calculated entropy generation by this model, the results of the entropy generation in the cavity was compared with the work of the Oliveski et al. [26] in figure 6. This figure shows the total entropy generation in the cavity verses Rayleigh number at different irreversibility distribution ratio, φ. Results show a good agreement with the previous results that shows the ability of this model to calculate of the entropy generation. Effect of the aspect ratio and Rayleigh number over the temperature distribution, flow field and entropy generation in Γ-shaped enclosure has been analyzed numerically using Lattice Boltzmann method at constant irreversibility coefficient($\psi=10^{-6}$). In this simulation the Rayleigh number and aspect ratio are changed from 10^3 to 10^6 and 0.25 to 3 respectively. Results are presented as a form of streamlines, temperature contours, entropy generation contours, mean Nusselt number and total entropy generation. Figure 7 shows the streamlines and temperature contours for AR=1(h=0.5, w=0.5) at different Rayleigh number. There exist two rotating cells in the enclosure. The main and the larger rotating cell on the left occupies region between left vertical wall and front face of the hot step which circulates counter clockwise (CCW). The small and secondary

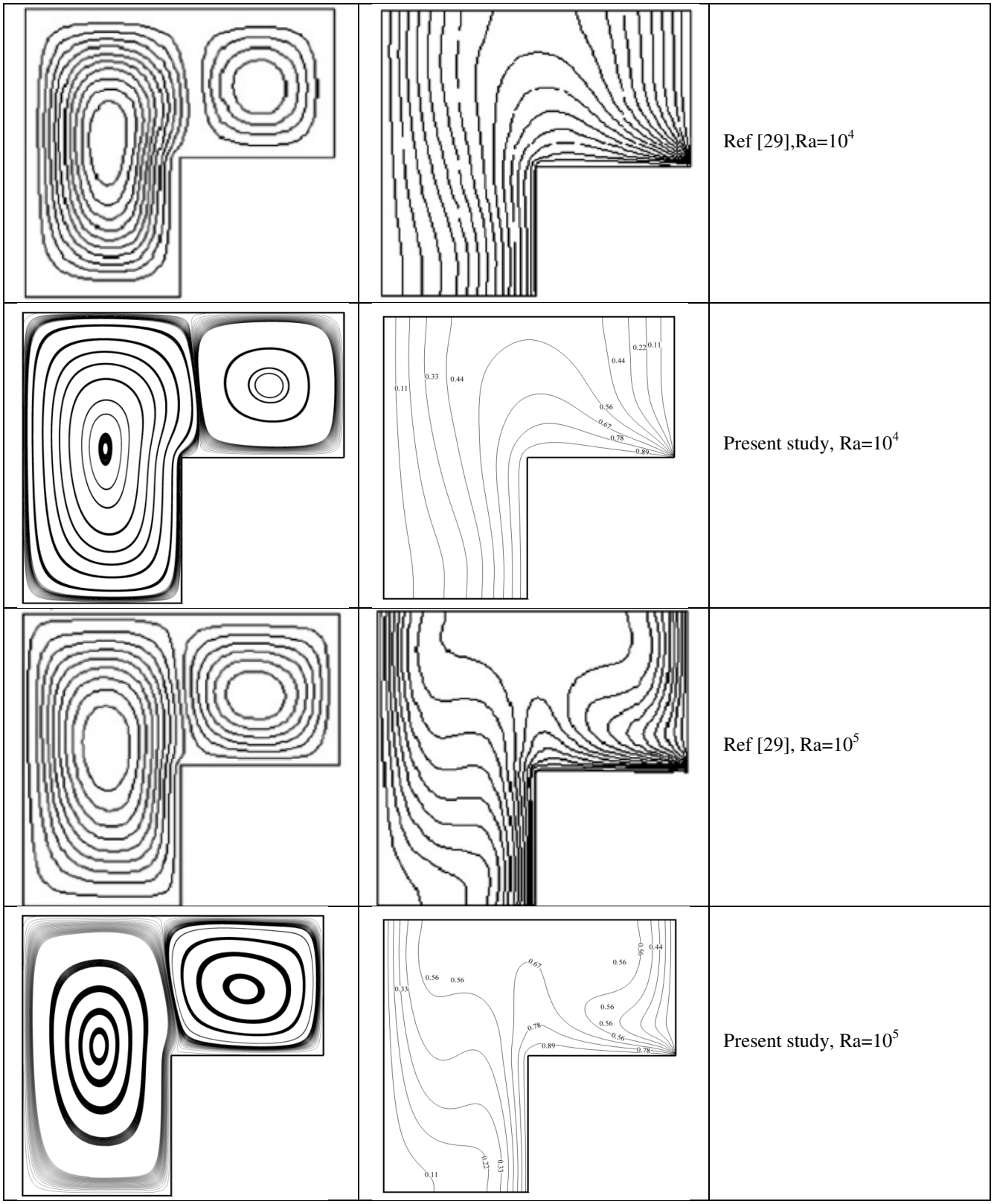


Fig. 5. Streamlines and temperature contours for different Rayleigh numbers in comparison with the FDM [29]

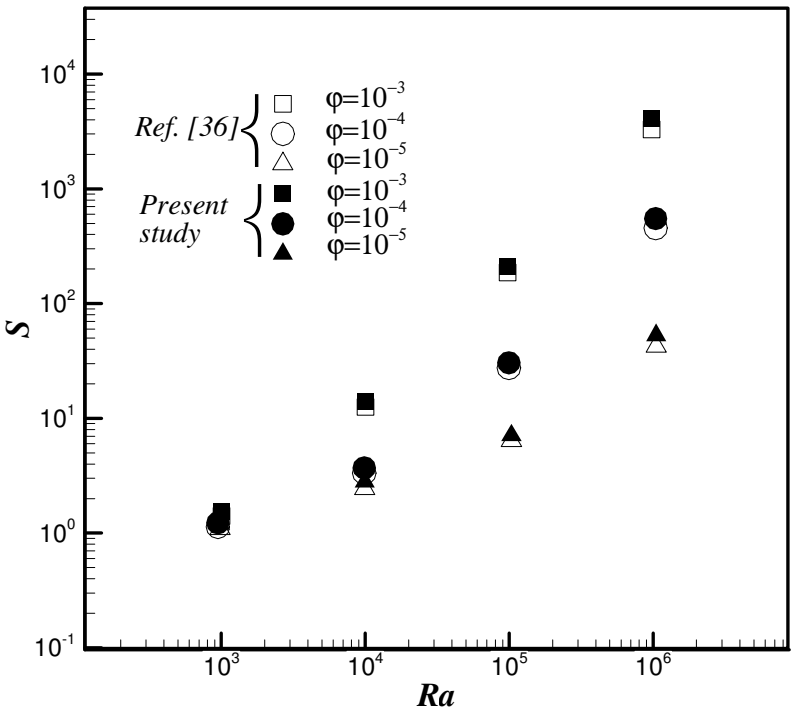


Fig. 6. Validation of total entropy generation in the square cavity in comparison with Ref [26]

Table 1.
The averaged Nusselt Number on the step's wall of Γ-shaped enclosure for different grid points

	Mesh size			
Ra	40×40	80×80	100×100	110×110
10^5	18.52	18.66	18.69	-
10^6	26.93	27.15	27.23	27.26

Table 2.
The averaged Nusselt Number on the vertical Boundary at x=0 in comparison with the previous study

Nu	Ref[25]	Present study	Ref[25]	Present study	Present study
Ra	40×40	40×40	80×80	80×80	100×100
10^5	4.487	4.449	4.523	4.508	4.512
10^6	8.798	8.623	8.928	8.883	8.891

cell forms over the step and circulates clockwise. At Ra=10^3, the heat transfer is mainly controlled by conduction. The isotherms are nearly parallel to the vertical wall which indicates domination of conduction heat transfer in this case. At Ra=10^5, the intensity of the circulation becomes stronger, which

implies that the convection heat transfer begins dominating the thermal flow field in the cavity. As the Rayleigh number becomes large ($Ra=10^6$), the crowded streamlines and isothermal lines indicate that the hydrodynamic and thermal boundary layers have been developed along the hot and cold walls**,** respectively, reflecting rigorous heat transfer rate occurred**.**

Variation of the flow field and temperature distribution has a different effect over the entropy generation. Figure 8 shows the contours of local entropy generation due to heat transfer and fluid friction at different Rayleigh number for AR=1(h=0.5, w=0.5) at $\varphi=10^{-6}$. A comparison of the entropy generation maps for heat transfer and fluid friction (Fig. 8a.) at $Ra=10^3$ confirms the less effect of the fluid flow on entropy generation since the strength of recirculation is relatively low. The entropy generation due to fluid friction and heat transfer is considerably high close to the step's hot walls. At higher Rayleigh number, buoyancy force and consequently the fluid flow effects increases, hence, the values of entropy generation due to fluid friction increase. This phenomenon can be observed near the walls of cavity with brighter color of the figure 8(c, d).One of the main parameters that have a major effect over the flow field and heat transfer distribution in the enclosure is the aspect ratio (AR). The effect of AR and length of horizontal and vertical walls of the enclosure over the flow field and temperature contours are shown in figures 9 and 10. It is observed that when the isotherm lines are parallel together, the main mechanism of the heat transfer is conduction (Fig 9a.). This phenomenon can be observed for the high length of the horizontal hot wall (h). If the distance between the hot step and cold wall increases, the convective effect on heat transfer rate will increase. By decreasing the length of vertical wall, the second cell (over the step) gets bigger, so the heat transfer rate increases (Fig. 10c.). It is observed from the temperature contours which show the more diffusion of the heat to the main flow. It should be mentioned that the constant aspect ratio can be created by different length of the horizontal and vertical walls of the enclosure. This variation on the height of the walls has a special effect on heat transfer rate which will be explain as follows.

The total entropy generation at various Rayleigh numbers for different aspect ratio is plotted in figure 11. For all cases, the total entropy generation increases with increasing Rayleigh number, though the rate of increase is different as seen in the figure 11. It is observed that, for Rayleigh number lower than 10^5 the effect of the aspect ratio on total entropy generation is insignificant but for greater Rayleigh number the total entropy generation is increased considerably. It is due to the formation of the recirculation areas and their speed which have a direct effect over the entropy generation due to fluid friction. The effect of the secondary recirculation area over the entropy generation due to the fluid friction is more important than the first bubble at high Rayleigh number. This is occurred at lower aspect ratio and length of the vertical hot wall (h).

One of the main parameters in natural convection in the cavity is the rate of the heat transfer. In this study, the variation of the mean Nusselt number over the step walls of the cavity verses aspect ratio is plotted at different Rayleigh number. With increasing the AR, the size of the secondary recirculation over the horizontal wall of the step reduces and fills the gap between the horizontal surface of the step and insulated wall of the cavity. This phenomenon reduces the effect of the convection so the Nusselt number decreases which is observed for all size of the h (Fig. 12). On the other hand, at lower AR, the first recirculation propagates in the cavity and fills commonly with second bubble the gap between thehorizontal surface of the step and insulated wall. This phenomenon increases the effect of the convective heat transfer in comparison with the conduction and subsequently causes to increase the Nusselt number. With increasing the Rayleigh number, the speed of the flow in the cavity increases, therefore the convective heat transfer increases. This increase in the rate of the heat transfer is shown at the mean Nusselt number curve. It should be mentioned that the best heat transfer was observed for AR less than unity at h=0.25. It is due to formation of the bubbles in the cavity which was explained above. With increasing the h form 0.25 to 0.75, the Nusselt number decreases approximately 72% at all Rayleigh numbers for AR=1. This result shows that the effect of the h on heat transfer is more important than the aspect ratio.

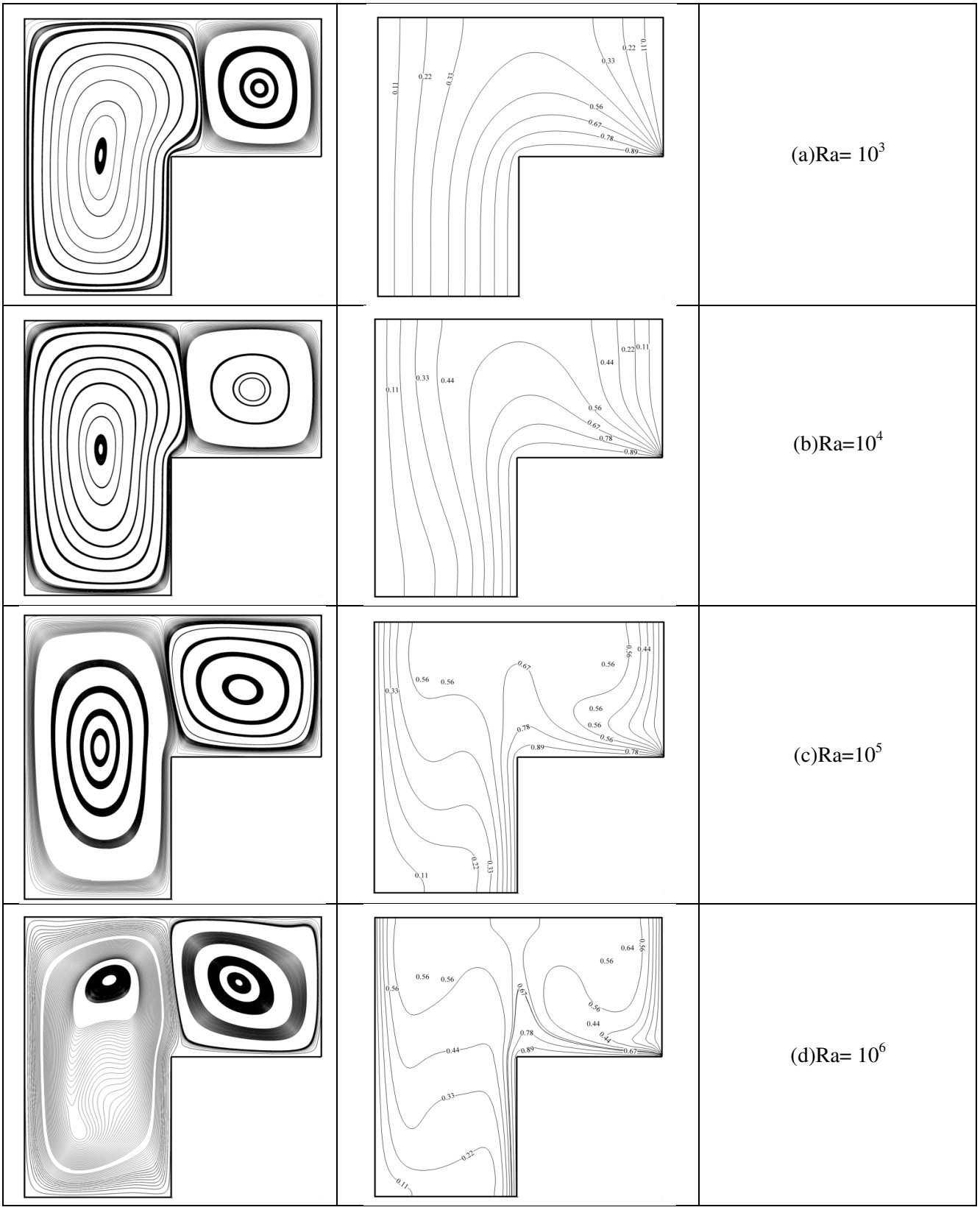


Fig. 7. Streamlines (top) and temperature contours (bottom) for h = w = 0.5 at different Rayleigh numbers

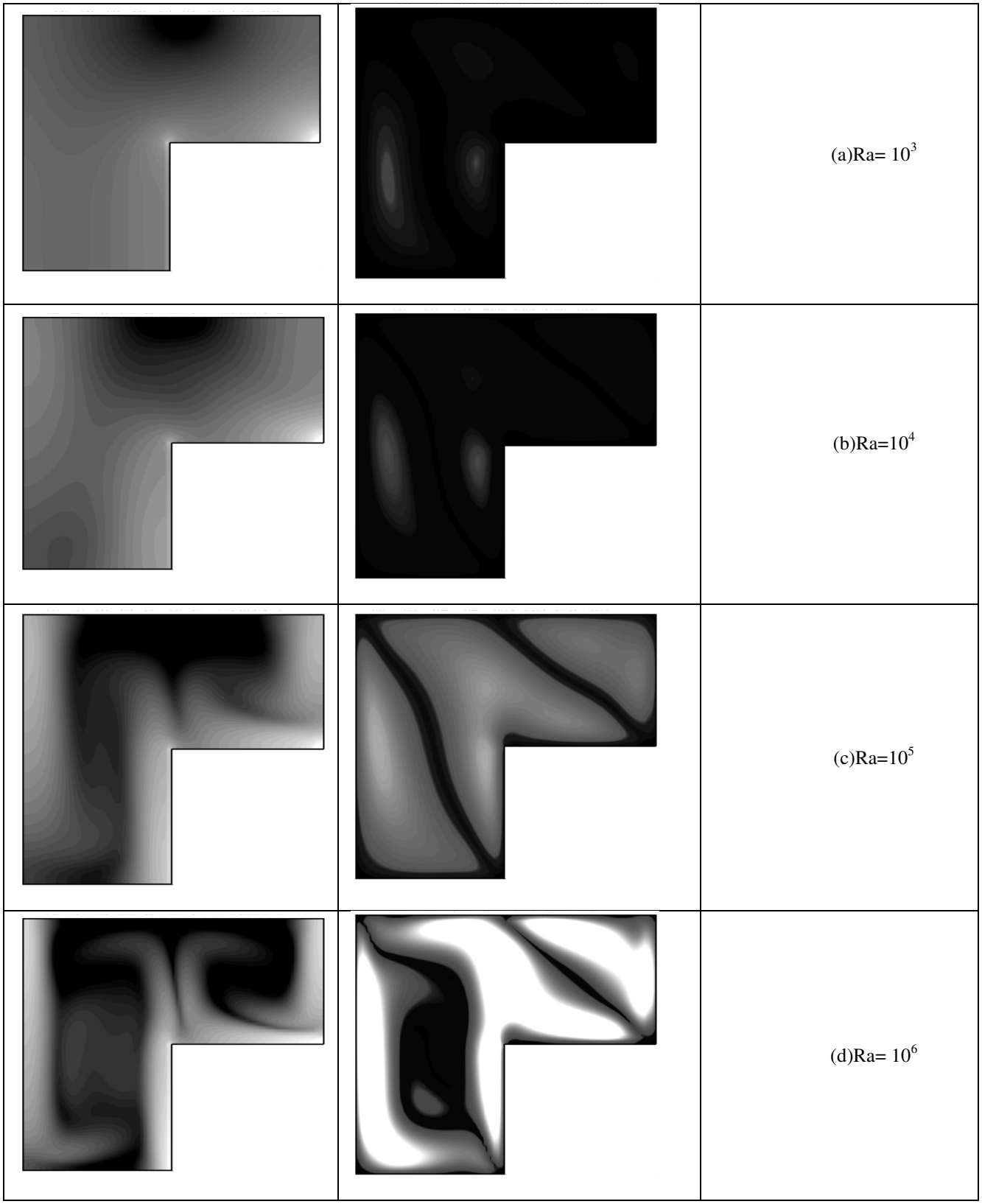


Fig. 8. Entropy generation due to heat transfer (on the top) and fluid friction (on the bottom) for h = w = 0.5 at different Rayleigh number

6. CONCLUSION

In this study the effect of aspect ratio and Rayleigh number on the heat transfer and entropy generation in the Γ-Shaped enclosure was investigated numerically using Lattice Boltzmann Method. The results of this study show that new model of the Kao et al. [32] for determining an appropriate characteristic velocity value based on the principle of kinetic theory is not only a suitable model for calculating the heat transfer characteristic but also a very useful technique to calculate the entropy generation in the natural convection problems. The accuracy of the present study for calculating the entropy generation in comparison with previous result [26] in the square cavity was very well. In Γ-Shaped enclosure, the numerical results show that increasing the Rayleigh number causes to increase the Nusselt number for all cases. At high aspect ratio, the formation of the bubbles causes to increase the diffusion heat transfer in comparison with convective heat transfer so Nusselt number decreases for all cases. The best heat transfer performance was observed at low AR. Also it was observed that the lowest size of the vertical wall of the step has a best heat transfer rate for low AR. The entropy generation is independent of the AR for low Rayleigh number which is due to the low speed of the fluid and subsequently low entropy generation due to the fluid friction. In natural convection in the cavity, the main part of the entropy generation was created by fluid friction so it was high at high Rayleigh number. The size of the vertical wall of the step does not have any observable effect on total entropy generation except for high Rayleigh number.

References

[1] Y.H Qian., D. d'Humieres, P. Lallemand, Lattice BGK models for Navier–Stokes equation, Europhys. Lett. 17 (6) (1992) 479–484.

[2] S. Chen, G.D. Doolen, Lattice Boltzmann method for fluid flows, Annu. Rev. Fluid Mech. 30 (1998) 329–364.

[3] D. Yu, R. Mei, L.S. Luo, W. Shyy, Viscous flow computations with the method of lattice Boltzmann equation, Progr. Aerospace Sci. 39 (2003) 329–367.

[4] S. Succi, The Lattice Boltzmann Equation for Fluid Dynamics and Beyond, Clarendon Press, Oxford, 2001.

[5] X. Shan, Simulation of Rayleigh–Benard convection using a lattice Boltzmann method, Phys. Rev. E 55 (1997) 2780–2788.

[6] X. He, S. Chen, G.D. Doolen, A novel thermal model for the lattice Boltzmann method in incompressible limit, J. Comput. Phys. 146 (1998) 282–300.

[7] Y. Zhou, R. Zhang, I. Staroselsky, H. Chen, Numerical simulation of laminar and turbulent buoyancy-driven flows using a lattice Boltzmann based algorithm, Int. J. Heat Mass Transfer 47 (2004) 4869–4879.

[8] H.N. Dixit, V. Babu, Simulations of high Rayleigh number natural convection in a square cavity using the lattice Boltzmann method, Int. J. Heat Mass Transfer 49 (2006) 727–739.

[9] P.H. Kao, R.-J. Yang, Simulating oscillatory flows in Rayleigh– Benard convection using the lattice Boltzmann method, Int. J. Heat Mass Transfer 50 (2007) 3315–3328.

[10] Y. Peng, C. Shu, Y.T.Chew, Simplified thermal lattice Boltzmann model for incompressible thermal flows, Phys. Rev. E 68 (2003) 026701.

[11] G. Barrios, R. Rechtman, J. Rojas, Tovar R., The lattice Boltzmann equation for natural convection in a two-dimensional cavity with a partially heated wall, J. Fluid Mech. 522 (2005) 91–100.

[12] A. Bejan, Heat Transfer, Wiley, New York, 1993.

[13] I. Catton, Natural Convection in Enclosures, Proc. the 6th Int. Heat Transfer Conference, 6 (1978) 13-31.

[14] S. Ostrach, Natural Convection in Enclosures, J. Heat Transfer 110 (1988) 1175-1190.

[15] S. Kakaç, Y. Yener, Convective Heat Transfer, CRC Press, 2nd ed. (1995) 340-350.

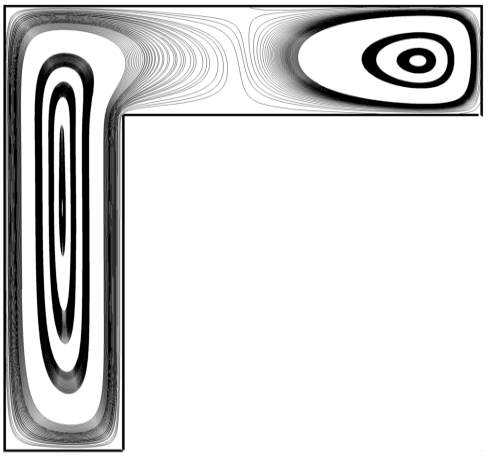
[16] D. Poilikakos, Natural convection in a confined fluid - filled space driven by a single vertical wall with warm and cold regions. J. Heat Transfer 107 (1985) 867-876.

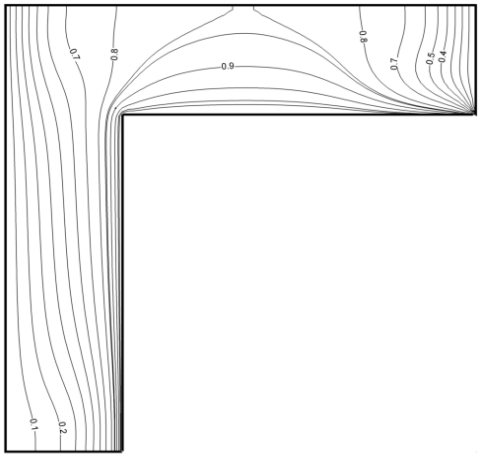
[17] D. Angirasa, M. J. B. M. Pourquié, F. T. M. Nieuwstadt, Numerical study of transient and steady laminar buoyancy - driven flows and heat transfer in a square open cavity. Numerical Heat Transfer Part A 22 (1992) 223-239.

[18] O. Ayhan, A. Ünal, T. Ayhan, Numerical solutions for buoyancy - driven flow in a 2-D square enclosure heated from one side and cooled from above, Advanced in Computational Heat Transfer, TR, (1997) 337–394.

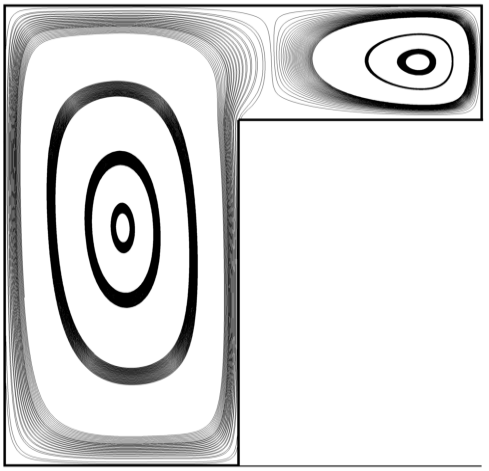
[19] K. Küblbeck, G. P. Merker, J. Straub, Advance numerical computation of two – dimensional time - dependent free convection in cavities. Int. J. Heat Mass Transfer 23 (1980) 203-217.

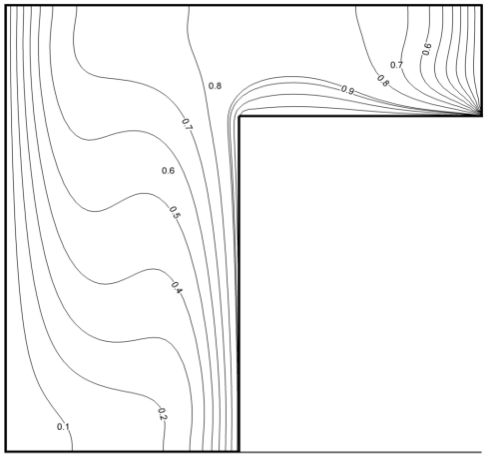
[20] N. C. Markatos, K. A. Pericleous, Laminer and turbulent natural convection in an enclosed cavity, Int. J. Heat Mass Transfer 27 (1984) 755-772.



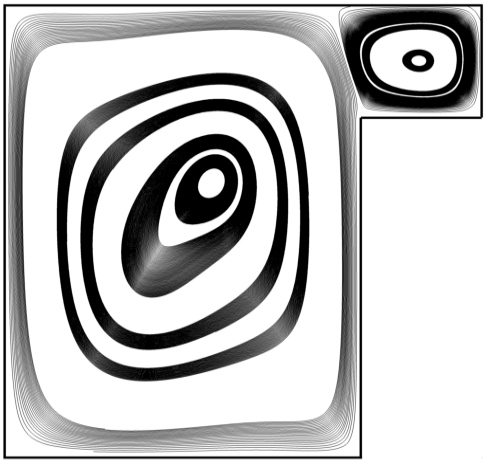


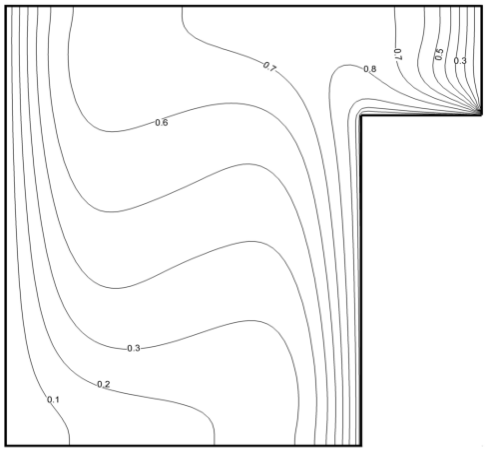
(a) h = 0.75,
(b) w = 0.75





(b)) h = 0.75,
w = 0 . 50





(c) h = 0.75,
w = 0.25

Fig. 9. Streamlines (on the top) and temperature contours (on the bottom) at Ra =10^5 for different Ar (h= constant).

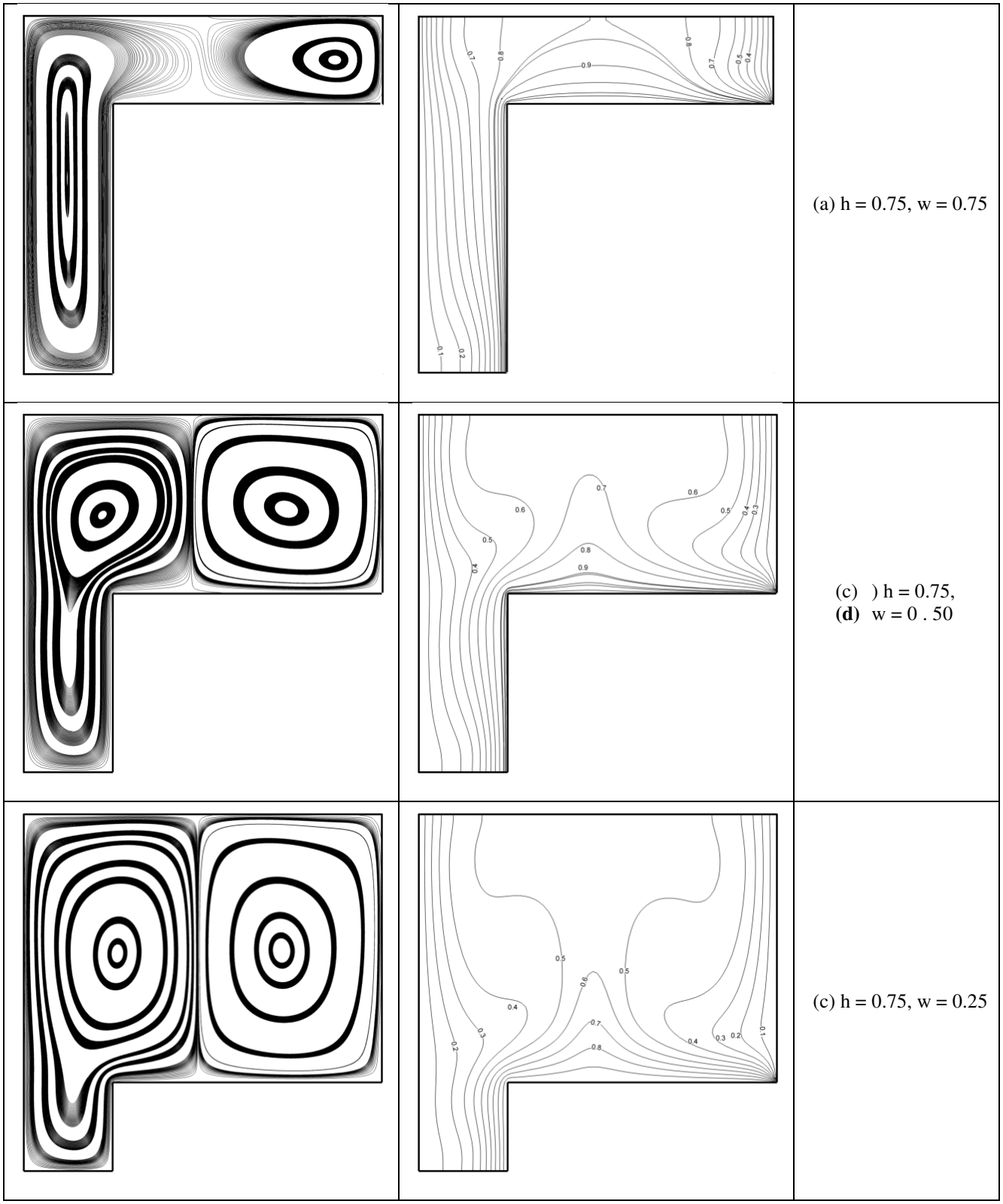


Fig. 10. Streamlines (on the top) and temperature contours (on the bottom) at Ra =10^5 for different Ar (w= constant).

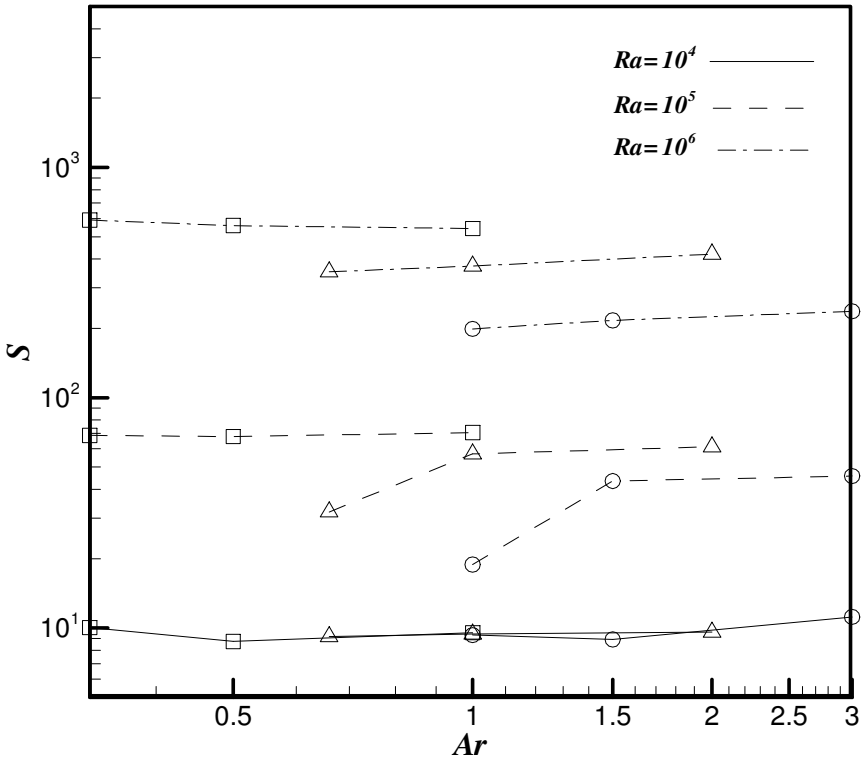


Fig. 11. Variation of the dimensionless total entropy generation with Ar at different Rayleigh number and φ=10^{-6}. (□) h=0.25, (Δ) h=0.5 and (O) h=0.75.

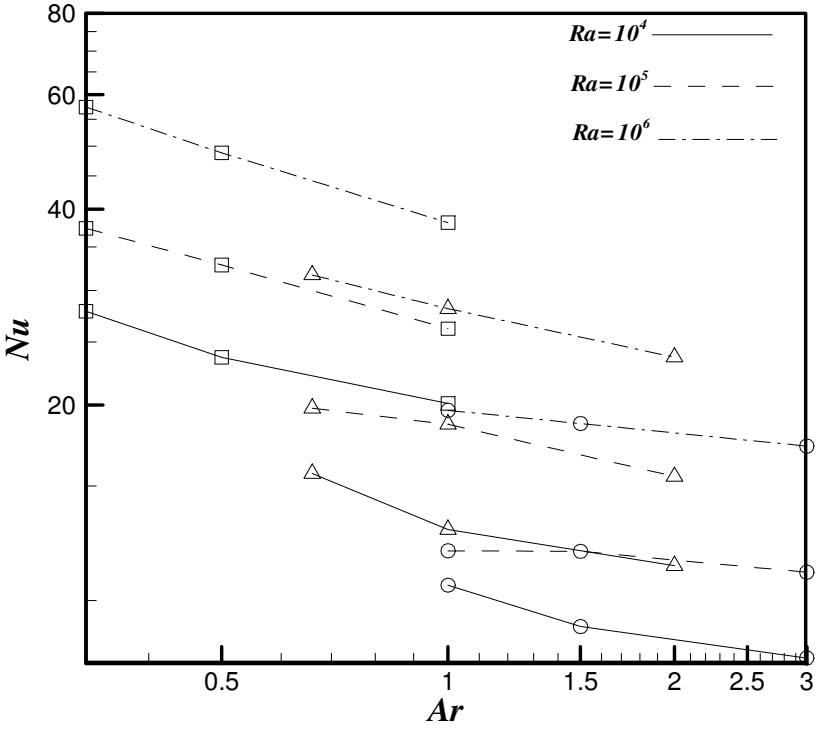


Fig. 12. Variation of mean Nusselt number with Ar at different Rayleigh number. (□) h=0.25, (Δ) h=0.5 and (O) h=0.75.

[21] L. Lage, A. Bejan, The Ra-Pr domain of laminar natural convection in an enclosure heated from the side. Numerical Heat Transfer Part A 19 (1991) 21-41.
[22] A. Bejan, Entropy generation through heat and fluid flow. New York: Wiley; 1982.
[23] A. Bejan, Entropy generation minimization. New York: CRC Press; 1996
[24] A. Bejan, Advanced engineering thermodynamics, 2nd ed. New York: Wiley
[25] G. de Vahl Davis, Natural convection of air in a square cavity: a bench mark numerical solution, Int. J. Numer. Methods Fluids. 3 (1983) 249–264.
[26] D. Rejane, C. Oliveski, H. Mario Macagnan, B. Jacqueline Copetti, Entropy generation and natural convection in rectangular cavities, J. Applied Thermal Engineering
[27] M.Y. Ha, M.J. Jung, A numerical study on three-dimensional conjugate heat transfer of natural convection and conduction in a differentially heated cubic enclosure with a heat-generating cubic conducting body, Int. J. Heat and Mass Tran. 43 (2000) 4229–4248.
[28] A. Mezrhab, H. Bouali, C. Abid, Modelling of combined radiative and convective heat transfer in an enclosure with a heat-generating conducting body, International Journal of Computational Methods 2 (3) (2005) 431–450.
[29] I. Dagtekin, H.F. Oztop, A. Bahloul., Entropy generation for natural convection in Γ-shaped enclosures, Int. Commun. Heat Mass Transf. 34 (2007) 502–510.
[30] P.H. Kao, Y.H. Chen, R.J. Yang, Simulations of the macroscopic and mesoscopic natural convection flows within rectangular cavities, J. Heat Mass Tran. 51 (2008) 3776–3793.
[31] Z. Guo, B. Shi, C. Zheng, A coupled lattice BGK model for the Boussinesq equations, Int. J. of Numerical Methods in Fluids, 39(4) (2002) 325-342.
[32] Z.L. Guo, Ch. Zheng, B.C. Shi, An extrapolation method for boundary conditions in lattice Boltzmann method, Phys. Fluids, 14 (6) (2002) 2007-2010.
[33] R. Mei, D. Yu, W. Shyy, L. Sh. Luo, Force evaluation in the lattice Boltzmann method involving curved geometry, Phys. Rev. E,.65 (2002) 1-14.
[34] Z.L. Guo, B.C. Shi, Ch. Zheng, A coupled lattice BGK model for the Boussinesq equations, Int. J. Numer. Methods Fluids, 39 (4) (2002), 325-342.
[35] E. K. Glapke, C.B. Watkins, J. N. Cannon, Constant heat flux solutions for natural convection between concentric and eccentric horizontal cylinders, Numer. Heat Transfer, 10 (1986), 279-295.
[36] X. He, Q. Zou, L.S. Luo, M. Dembo, Analytic solutions of simple flows and analysis of nonslip boundary condition for the lattice Boltzmann BGK model, J. Stat. Phys. 87 (1997), pp. 115–136.
[37] H.N. Dixit, Simulation of flow and temperature fields in enclosures using the lattice Boltzmann method. MS Thesis, 2005, Indian Institute of Technology Madras, India.
[38] Z.L. Guo, Ch. Zheng, B.C. Shi, An extrapolation method for boundary conditions in lattice Boltzmann method, Phys. Fluids, 14 (6) (2002), 2007-2010.
[39] C. Cercignani, Mathematical Methods in Kinetic Theory, Plenum, New York, 1969.
[40] G. Wannier, Statistical Physics, Diver, New York, 1966.
[41] C. Shu, X.D. Niu, Y.T. Chew, A lattice Boltzmann kinetic model for microflow and heat transfer, J. Stat. Phys. 121 (1–2) (2005) 239–255